

Improving the precision of irrigation in a pistachio farm using an unmanned airborne thermal system

V. Gonzalez-Dugo · D. Goldhamer · P. J. Zarco-Tejada · E. Fereres

Received: 11 November 2013 / Accepted: 9 September 2014 / Published online: 24 September 2014
© Springer-Verlag Berlin Heidelberg 2014

Abstract A study was conducted in a large pistachio farm in Madera County, California, to assess the spatial variability in water status and irrigation needs by using high-resolution thermal imagery acquired by an unmanned aerial system. We determined the Crop Water Stress Index (CWSI) of two fields, 130 ha each, based on canopy temperature measurements of individual tree crowns, thus assessing the spatial variations in tree water status within each field. The CWSI of each potential management unit (sectors encompassing about 175 trees) was then calculated and related to the days since last irrigation (DSL) in F1 and F2. The relationship between CWSI and DSL was established to calculate the average CWSI corresponding to the whole area that was irrigated on the same day. This value was afterward compared with the actual CWSI value of each management unit as a proxy of the spatial variability in CWSI. This information was used to calculate the deviation of each irrigation unit from the fixed irrigation schedule for the whole fields. Our results show that it is feasible to use high-resolution thermal imagery for integrating the

crop response in irrigation performance assessment and for providing recommendations at the farm scale.

Introduction

Irrigated agriculture is the main consumer of freshwater globally. Efficient use of water in agriculture is a requisite to release water resources to other sectors of society where demand is increasing (Jury and Vaux 2007). The prospects of water scarcity are increasing in many world areas (Molden 2007) adding more pressure for irrigated agriculture to minimize water losses and maximize water productivity. Improvements in the engineering of pressurized irrigation systems (sprinkler and drip) have led to better distribution uniformities of applied water. This potentially decreases the number of underirrigated and overirrigated plants, thereby improving irrigation water productivity by maximizing the fraction of applied water that is consumed by the plants while minimizing potential losses to runoff and deep percolation (Evans and Sadler 2008). Drip and microsprinkler irrigation systems have also improved water productivity by potentially decreasing the amount of water lost to surface evaporation (Bresler 1977; Bonachela et al. 2001). Advances in irrigation scheduling technologies, including matching applied water to consumptive use (ET_c), have also improved on-farm water productivity. The desirable irrigation system should apply precisely the prescribed amounts depending on the production capacity of each plot (Martin et al. 1990). None of the improvements in irrigation system design and operation address the issues of soil and plant heterogeneity and associated variations in water demand within irrigation management units. To decrease labor inputs and simplify management, there has been a tendency in recent decades toward increasing the

Communicated by B. Evans.

V. Gonzalez-Dugo (✉) · P. J. Zarco-Tejada · E. Fereres
Instituto de Agricultura Sostenible (IAS), Consejo Superior de
Investigaciones Científicas (CSIC), Alameda del Obispo s/n,
14004 Córdoba, Spain
e-mail: victoria.gonzalez@ias.csic.es

D. Goldhamer
Department of Land, Air and Water Resources, University
of California, Davis, CA 95616, USA

E. Fereres
Departamento de Agronomía, Universidad de Córdoba, Campus
Universitario de Rabanales, 14014 Córdoba, Spain

size of management units; this increases the risk of wider spatial variation within units. One of the first studies of spatial variation in crop response to irrigation was conducted by Sadler et al. (2002). They found unexpectedly wide variations in optimal irrigation amounts within irrigation blocks that they attributed primarily to differences in soil types and suggested that designers should reduce the size of the management units.

In addition to different soil types within management units, other sources of variation include microadvective effects, soil transport properties, soil depth, topography, salinity, plant size, weed cover, plant health (pests and diseases) and the aforementioned distribution of applied water (Zhang et al. 2002; Kravchenko et al. 2005; Rodriguez et al. 2009; Lee et al. 2010). While some of these sources of variation are static, others vary not only in space but also in time. Managing the variability can be achieved by two approaches: the map-based approach and the sensor-based approach (Zhang et al. 2002). Traditional approaches to system design have primarily minimized differences in soil type and topography within irrigation units. This can be done with the map-based approach. However, the myriad of the other sources of variation have been mostly ignored in system design and operation, in part, because they are dynamic and difficult to quantify. Once optimized, the sensor-based approach, with the required resolution and turnaround time, could provide an efficient tool to assess dynamic variations within agricultural fields. Previous works have demonstrated that thermal sensors installed onboard unmanned vehicles and systems (UAV, UAS) or manned aircrafts fulfill the requested accuracy and flexibility to deal with the dynamic variability (Peters and Evett 2004; Gonzalez-Dugo et al. 2013; Bellvert et al. 2014).

The main objective of farming—maximum profit and production with minimal inputs—is directly affected by plant uniformity. While characterizing heterogeneity in the field based on soil and irrigation system factors is currently used in system design and management, the plant should be the best indicator of its well-being. Moreover, since yield and crop quality are largely determined by plant water status, it follows that spatial assessment of plant water status can be a valuable indicator in system design and operation. Unfortunately, the current state of the art in plant water status monitoring, the pressure chamber, must be operated manually and is time consuming (Hsiao 1990). While one can make point observations to characterize the water status of single plants, it is impractical to use the pressure chamber to adequately quantify the plant water status of entire irrigation units.

Recent advances in remote sensing make accurate characterization of plant water status over irrigation units possible and practical (Ambast et al. 2002; Berni et al. 2009a; Gonzalez-Dugo et al. 2013). Canopy temperature is closely

related to plant transpiration and, thus, the overall plant water balance. Water deficits increase canopy temperatures, leading to the development of water stress indicators proposed long ago (Jackson et al. 1977). The most widely used indicator derived from thermal information is the Crop Water Stress Index (CWSI) where the canopy–air temperature difference is normalized by the evaporative demand (Idso et al. 1981). The temperature-derived indicators were developed originally with information obtained from handheld infrared thermometers, either used directly or mounted on a mast over the canopy. These point assessments do not allow for analysis of the spatial distribution of water status within a field. Aerial assessment, usually accomplished with aircraft or satellites, overcomes this problem. However, insufficient spatial resolution in the thermal domain from satellite imaging is normally a limitation, especially with discontinuous canopies found in orchards and vineyards where bare soil affects the retrieval of canopy temperature in aggregated pixels (Moran et al. 1994). For discontinuous canopies, aircraft can be flown at optimum elevations to insure the acquisition of high-resolution imagery as a function of the existing thermal detectors (i.e., sub-meter resolutions), allowing for the exclusion of all pixels other than vegetation from the calculation of canopy temperature (Berni et al. 2009a; Gonzalez-Dugo et al. 2012; Zarco-Tejada et al. 2013).

Several questions come up in considering the use of thermal images to assist irrigation management. The image represents the state of a field at a certain time—a snapshot—but plant water status normally changes between irrigations, in particular with low-frequency systems. A snapshot would indicate the instantaneous water status on that date and be useful to characterize variability at that time as well as for detecting leaks and other problems of the irrigation system. The question raised is how useful this single image is to predict the evolution of water status with time using systems that operate infrequently, such as sprinklers. Also, the issue of how consistent would be a sequence of images in characterizing the water status of a field remains unanswered. Clearly, the time-course development of canopy temperature determined with measurements on separate days within an irrigation cycle would provide better information than a snapshot. However, each image collection comes at a cost in flight, operation and processing even when low-cost solutions based on unmanned vehicles are used. Determining the frequency of thermal image acquisition is of paramount importance in using these techniques for practical irrigation management.

We conducted an experiment at a large, microsprinkler-irrigated, commercial pistachio farm by acquiring high-resolution thermal images over two irrigation blocks (130 ha each), each irrigated with a different frequency. The objectives were to a) assess the spatial heterogeneity in water

status and water needs within the two irrigation blocks and b) test a methodology based on the rate of change in CWSI that would predict the evolution of water status with time, thus anticipating the variations in irrigation needs within the management units of each field.

Materials and methods

Field site description

The study was carried out in a commercial pistachio orchard located in Madera County, CA, USA (36°58'N, 119°57'W), 75-m elevation on July 1 and 3, 2009. Pistachio trees (*Pistachia vera* cv. Kerman) were planted on 1994 in a triangular grid at a spacing of 5.8 m × 5.2 m (330 trees ha⁻¹). Tree canopies covered 55 % of the soil. The climate is Mediterranean, characterized by mild, rainy winters and hot, dry summers. The climatic conditions on the two measurement dates were very similar, clear days with an air temperature of 33 °C and a vapor pressure deficit of 3.5 kPa at the time of both flights. The irrigation method is full coverage with microsprinklers (model SVM516, Toro Ag, El Cajon, CA) in the rows located midway between the trees. At an operating pressure of 0.10 MPa, the microsprinkler average discharge was about 81.4 l h⁻¹ distributed over an effective wetting diameter of approximately 8.3 m. Further information concerning soil type and field description can be found in Iniesta et al. (2008) and Testi et al. (2008).

The entire commercial farming operation comprised about 1000 ha and is divided into fields of 800 × 1600 m or about 130 ha each. Two fields were chosen for the study. Each field comprised four different blocks (10,500 trees per block) where ten irrigation sets are run, one per block and day in a 10-day cycle daily (Fig. 1). Each set includes 7 rows of trees with about 150 trees per row. Each set is thus divided into six units controlled by individual valves which are run simultaneously for 24 h, applying a depth of 63 mm of water which we will refer to as the ranch practice. This amount was calculated according to the grower experience and the water availability. Although the set (gathering around 1,050 trees) is the management unit for the ranch practice, here we will consider the sector (175 trees) as our irrigation unit, as it is controlled by a valve which could eventually receive remote control signals and operate autonomously. Thus, the term “irrigation unit” is used hereafter to refer to sectors. One field (F1) was irrigated according to the farm schedule. In the other field (F2), the schedule was as in F1, until it was altered 16 days before the experiment started on July 1, with the goal of increasing the range of tree water status in different parts of the 130-ha field. In this second field (F2), irrigation was launched with the same dose as in F1 but every 2 days

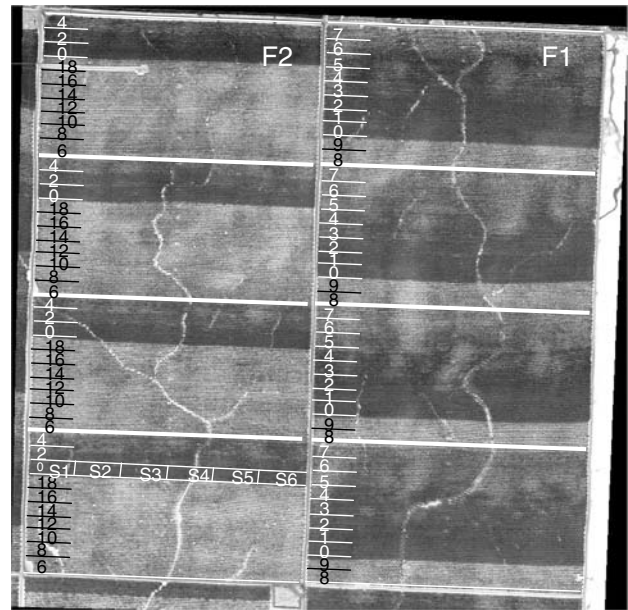


Fig. 1 Thermal mosaic of the two fields of the study acquired on July 3. For each set, the number of days elapsed since last irrigation is indicated on the *left* corner. As an illustration, the distribution of the six sectors comprised in an individual set is also shown

instead of daily, leading to an irrigation interval of 20 days with a spread of days since last irrigation ranging from two up to 18 days, at 2-day intervals. Thus, in F2, there were trees where the previous irrigation was applied from 0 to 18 days since last irrigation (DSL), while in F1, the DSL ranged from 0 to 9 days. Figure 1 depicts numerically the distribution of DSL on July 1 in the different sections of each of the two fields.

Airborne imagery

A thermal camera (Miracle 307 k, Thermoteknix Systems Ltd, Cambridge, UK) was installed on an unmanned airborne platform, as described by Zarco-Tejada et al. (2012, 2013) and flown over the experimental orchard on July 1 and 3, 2009 at 250 m above the ground level at solar noon. The camera had a resolution of 640 × 480 pixels with a field of view of 45° that delivered a ground resolution of 35 cm. The images were stored on board in a raw format with 16-bit radiometric resolution, processed as described by Zarco-Tejada et al. (2012, 2013) and calibrated using ground temperature data collected during each flight. Black and white ground references as well as soil targets were measured during each flight with a handheld infrared thermometer (LaserSight, Optris, Germany).

Mean crown temperature (T_c) was obtained for every tree crown within each unit (between 170 and 180 trees per unit), for a total of about 42,900 trees in each of the

two studied fields. The T_c values were used to calculate the CWSI as described below.

Determination of the Crop Water Stress Index

The Crop Water Stress Index (CWSI) was determined according to Idso et al. (1981) as follows:

$$\text{CWSI} = \frac{(T_c - T_a) - (T_c - T_a)_{LL}}{(T_c - T_a)_{UL} - (T_c - T_a)_{LL}} \quad (1)$$

where $(T_c - T_a)$ is the difference between canopy and air temperature and subscripts LL and UL correspond to the lower and upper limit, respectively. The lower limit is established by the non-water-stressed baseline (NWSB) that is developed from the $T_c - T_a$ values of a canopy transpiring at its maximum rate for a given vapor pressure deficit (VPD). In this case, we used a NWSB previously obtained for pistachio in the same orchard using infrared thermometers installed approximately 1 m over the canopy ($T_c - T_a = -1.33 \text{ VPD} + 2.44$, $R^2 = 0.87$; Testi et al. 2008). The NWSB was determined from DOY 164 to DOY 264, thus covering the irrigation season for the species. CWSI varies between 0 and 1, although given the dispersion of the experimental points around the NWSB regression line (Testi et al. 2008), numbers below the theoretical lowest CWSI value of zero should be expected here. The upper limit corresponds with the $T_c - T_a$ value of a canopy where the transpiration is completely halted and was determined according to the methodology proposed by Idso et al. (1981), where the UL corresponds to the $T_c - T_a$ calculated for the VPD that exists between the foliage and the air for the empirically observed temperature difference at $\text{VPD} = 0$. The CWSI value of every unit was computed by averaging the CWSI of individual tree crowns for the 160–170 trees of each unit.

Once the actual CWSI was determined for each unit (CWSI_a), the values were related to the days elapsed since last irrigation to compute the average value corresponding to each time step (day). In a perfectly uniform field, all management units that were irrigated on the same day should have the same CWSI (denominated henceforth as $\overline{\text{CWSI}}$). Then, we calculated the deviation of the CWSI of each individual unit from the $\overline{\text{CWSI}}$ of the sets that were irrigated on the same day.

Tree water relation measurements

Five trees were randomly selected from each set in one of the four replicate blocks of F2 to evaluate tree water status. Tree water status was assessed by measuring shaded leaf water potential (SWP, MPa) with a pressure chamber (Model 3005, SoilMoisture Equipment Co., Santa Barbara, CA, USA). Shaded leaves located near the trunk

were chosen according to the methodology described in Goldhamer and Fereres (2001). Stomatal conductance (G_s , $\text{mmol m}^{-2} \text{ s}^{-1}$) was measured with a leaf porometer (SC-1, Decagon Devices, Pullman, WA, USA) on two trees located in irrigation sets that corresponded with 4, 8, 16 and 18 DSLI. Measurements were carried out on July 1 and July 3; thus, the trees selected for measurements differed between the two dates, according to the shift in the irrigation schedule.

Triggering the spatial variability in a rotational system

Given the irrigation system of the orchard, the analysis of the spatial variability must take into consideration the time elapsed since last irrigation, i.e., from 0 to 9 DSLI in F1 and from 0 to 18 DSLI in F2. Considering the four blocks per field, the 10 sets per block and the six units per set, a total of 24 units are being irrigated on any single day. To obtain an $\overline{\text{CWSI}}$ for that day, the values for the 24 units were averaged for each of the 10 time steps considered (see Fig. 1) to develop a relationship between the average CWSI thus calculated and DSLI. The spatial variability was then assessed by comparing, for any given DSLI, the individual CWSI value of any unit against the average CWSI.

Once the relationship between CWSI and DSLI was calculated, it was then inverted to assess the spatial variability in time units (days), instead of CWSI values. Hence, once the map of the bias in $\overline{\text{CWSI}}$ of all the units was established, the bias from the $\overline{\text{CWSI}}$ was converted to bias in days, indicating the deviation in days of the ideal irrigation schedule of each unit from the 10-day fixed schedule. The added value of this analysis is that it offers a framework for comparing fixed versus variable scheduling for irrigation management.

Results

The interpolated map of the CWSI for both fields, F1 and F2, calculated after the individual crown data of every single tree is shown in Fig. 2. The CWSI values in F2 were generally higher (evidenced by the red color) due to its longer irrigation interval (20 days). The range of variability among sets and within units of the same set can be inferred from the two images in Fig. 2.

The mean value of CWSI and its standard deviation were calculated for each of the different potential irrigation units that may be considered, i.e., tree, unit, set and block levels (Table 1). The number of trees that were analyzed at each level is also reported in Table 1. It can be observed that, although the mean value changed little, the standard deviation decreased as the number of considered trees increased.

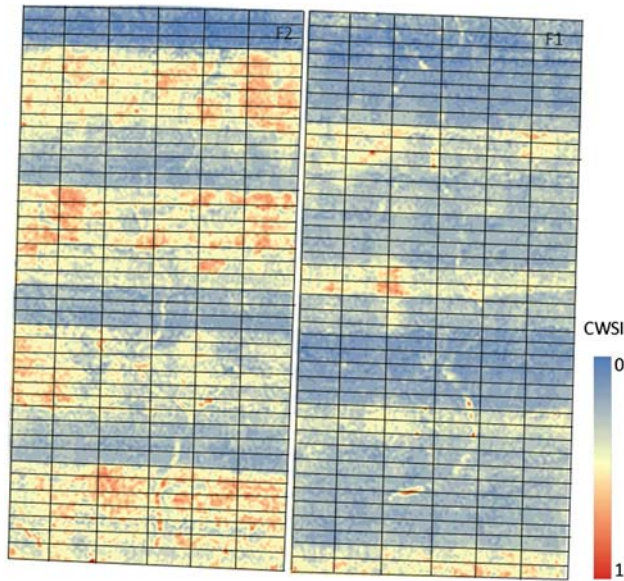


Fig. 2 Map of CWSI values for the *F1* field (10-day schedule; *right*) and the *F2* field (20-day schedule, *left*) obtained at 13.00 h on July 3 (color figure online)

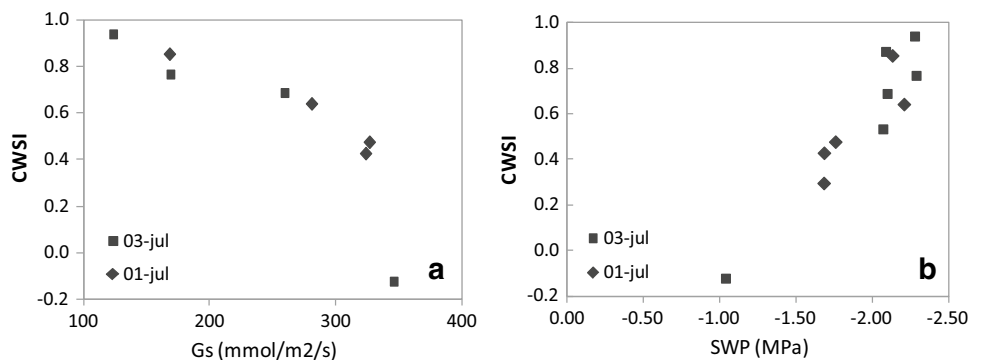
Table 1 Mean value of the Crop Water Stress Index (CWSI) and its SD calculated at the tree, sector, set and block level on July, 1st

Potential irrigation units	# Trees	CWSI F1	CWSI F2
Individual tree	–	0.29 ± 0.46	0.52 ± 0.48
Unit	175	0.29 ± 0.41	0.54 ± 0.37
Set	1,050	0.29 ± 0.40	0.53 ± 0.33
Block	10,500	0.29 ± 0.13	0.53 ± 0.21

Trees that were irrigated the same day of the image acquisition or 2 days before were excluded for the analysis. The number of trees grouped at each scale is also shown

Figure 3 shows that measurements of CWSI correlated well with point measurements of water potential (SWP) and stomatal conductance (G_s) taken in F2. Stomatal conductance was maintained at values around $350 \text{ mmol m}^{-2} \text{ s}^{-1}$ until CWSI reached 0.5. From that CWSI threshold, G_s decreased almost linearly (Fig. 3a). The relationship

Fig. 3 Relationship between CWSI and, **a** stomatal conductance (G_s ; $\text{mmol m}^{-2} \text{ s}^{-1}$), and **b** stem water potential (SWP; MPa) measured in *F2* on both dates



between CWSI and SWP was linear for the range of data collected in F2 (Fig. 3b). Figure 4a, b depicts the relationships between CWSI and DSLI observed in F1 and F2 and obtained in the two different flights, respectively. The observed patterns were very similar for the 2 days, with mean CWSI values varying between -0.2 and 0.8 for F2 and between -0.2 and 0.6 for F1. In F1, calculated CWSI remained below zero until 5 DSLI. After 5 days, CWSI increased sharply reaching a value between 0.6 and 0.8 on 10 DSLI. In F2, CWSI rose earlier than in F1, just after 2–4 DSLI (Fig. 4). It increased at a similar rate as in F1, reaching an average value of CWSI approaching 0.8 on 10–12 DSLI, and then stayed around the same level until 18 DSLI on both dates (Fig. 4).

The change in the slope of the CWSI versus time relationships should be indicative of the dynamics of stress development. Figure 5 compares the trends in change in the slope of CWSI between both fields, which were somewhat different. In F2, the slopes were much higher until day five and then decreased as time went on. In F1, the magnitude of the slopes was less but the trend was similar (Fig. 5). In both fields, the slope of the CWSI with time became nil or negative for the last sets prior to irrigation.

Figure 6 shows the relative distribution of the CWSI based on the aggregation of the individual irrigation units of F2. Four lines are depicted in Fig. 6 corresponding to the cumulative distribution of the CWSI of units that had been irrigated 6, 8, 10 and 16 days before. The lines in Fig. 6 may be used to determine the percentage of the area that remained below a specified CWSI threshold. As an example, CWSI thresholds of 0.5 and 0.8 are marked in Fig. 6 as indicative values of moderate and severe stress levels, respectively. These values were established according to the relationship between CWSI and SWP displayed in Fig. 4. It can be observed that nearly 30 % of those sectors in F2 that were irrigated 6 days before were above the moderate CWSI threshold. By contrast, 90 % of the area irrigated 10 days before was already beyond that threshold. Distributions for the units last irrigated 10 and 16 days were similar and showed that over 35 % of the whole F2 field was already above the severe CWSI threshold (Fig. 6).

Fig. 4 Evolution of CWSI with time in F1 and F2 for July 1 (a) and July 3 (b)

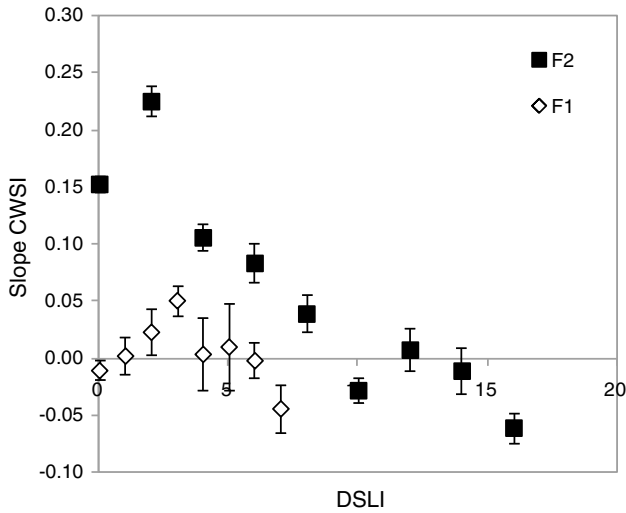
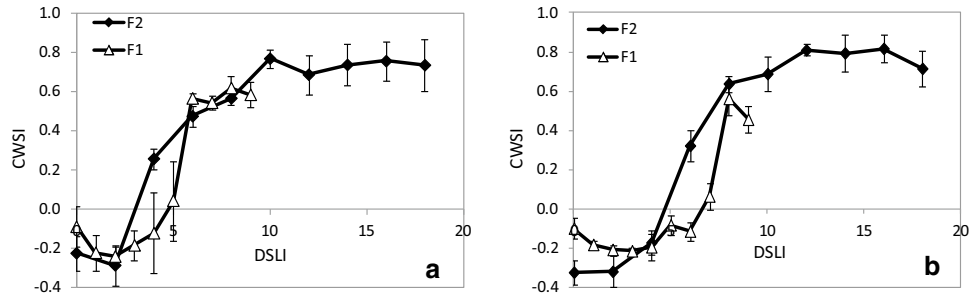


Fig. 5 Evolution of the CWSI slope from 1 to 3 July in F1 and F2 as a function of days since last irrigation (DSLl) on the first day of measurement

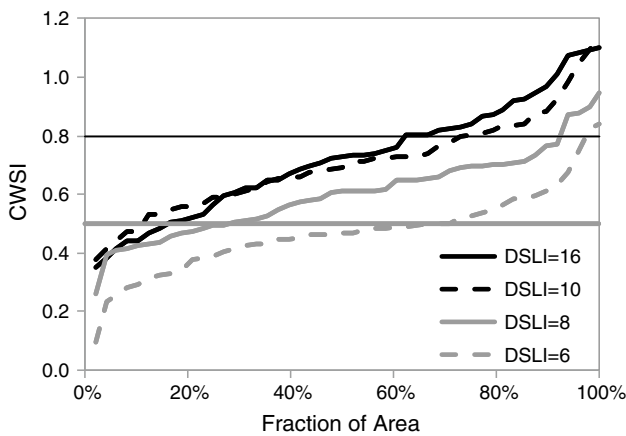


Fig. 6 Cumulative area distribution of CWSI for different days after irrigation with two different CWSI thresholds in F2

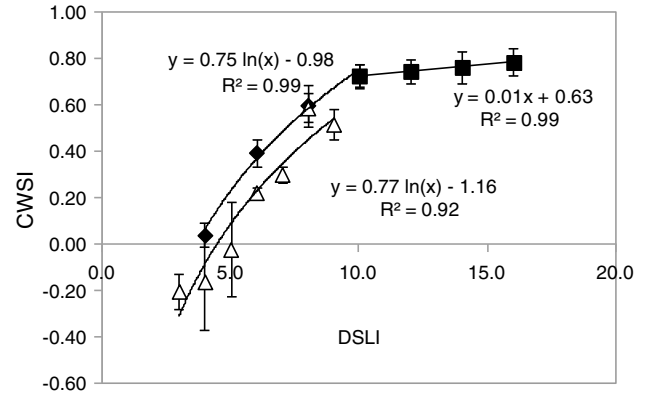
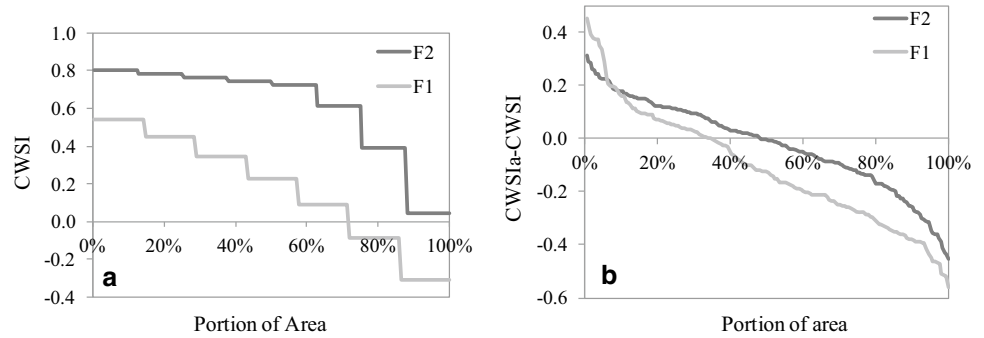


Fig. 7 Relationships between days since last irrigation and average CWSI for each field, F1 (open symbols) and F2 (closed symbols). For F2, two regression functions were adjusted, corresponding to the period from 0 to 10 DSLI (solid diamonds) and from 10 to 16 DSLI (solid squares). Vertical bars show the SE ($n = 48$)

Given the consistency observed between the CWSI determinations on July 1 and July 3 (Fig. 4), we averaged the CWSI of each irrigation unit, according to the time that had passed since last irrigation. Therefore, a mean CWSI value for the 48 sectors (24 sectors over the two dates) with the same DSLI was obtained and plotted against DSLI as in Fig. 7, for F1 and F2. Irrigation units that were irrigated on the day of measurement, and one or 2 days before were excluded from the analysis, as the small differences between the wet soil and crowns decreased the accuracy of the automated identification of the tree crowns within the images. For days three to 10, the relationship is nearly identical in F1 and F2, except that they run parallel to each other, with an equivalent distance of one to 2 days (Fig. 7). In the case of F2, the data fitted two different regressions, one between day three and 10 and another for days 10 to 18.

The relationships of Fig. 7 allowed the determination of the theoretical CWSI that should correspond to each set

Fig. 8 **a** Average CWSI (\overline{CWSI}) of each unit (obtained from Fig. 7) as a function of cumulative area for *F1* and *F2*; and **b** calculated deviation of the CWSI for each valve from the average value (calculated as a function of the days since irrigation) as a function of cumulative area for *F1* and *F2*



based on the time elapsed since last irrigation. The \overline{CWSI} for every DSLI was thus obtained, and the cumulative distribution of the \overline{CWSI} according to the time elapsed since irrigation for both fields, F1 and F2, was calculated and is shown in Fig. 8a. The *CWSI* may be then compared against the actual measured *CWSI* ($CWSI_a$) of each unit (calculated from the actual *Tc* reported in the maps of Fig. 2). The difference between $CWSI_a$ and \overline{CWSI} could be used as a proxy to assess the spatial heterogeneity. Positive values of $CWSI_a - \overline{CWSI}$ indicate that the unit is more stressed relative to what it should have been, given its time since last irrigation. On the contrary, negative $CWSI_a - \overline{CWSI}$ values indicate plots that are less stressed than what should be expected from the irrigation sequence. After the calculations of $CWSI_a - \overline{CWSI}$ were performed for each irrigation unit, they were plotted against the area to obtain a distribution function, as shown in Fig. 8b. By inverting Fig. 7 relationships and calculating the equivalent in days to a change in *CWSI*, the bias in *CWSI* of each unit relative to the theoretical irrigation sequence of each unit. For instance, a $CWSI_a - \overline{CWSI}$ of 0.17 is equivalent to 1 day (Fig. 7).

Figure 9 shows the spatial distribution of the deviations of each irrigation unit, in terms of days, from the irrigation interval of the standard 10-day (F1) or 20-day (F2) schedules. Plots corresponding to those units that were irrigated 2 days (or less) prior to the measurements were not included in the analysis. From the data in Fig. 9, it is possible to recommend an optimal irrigation interval for each irrigation unit within the field, which would be different from the fixed time interval for each field.

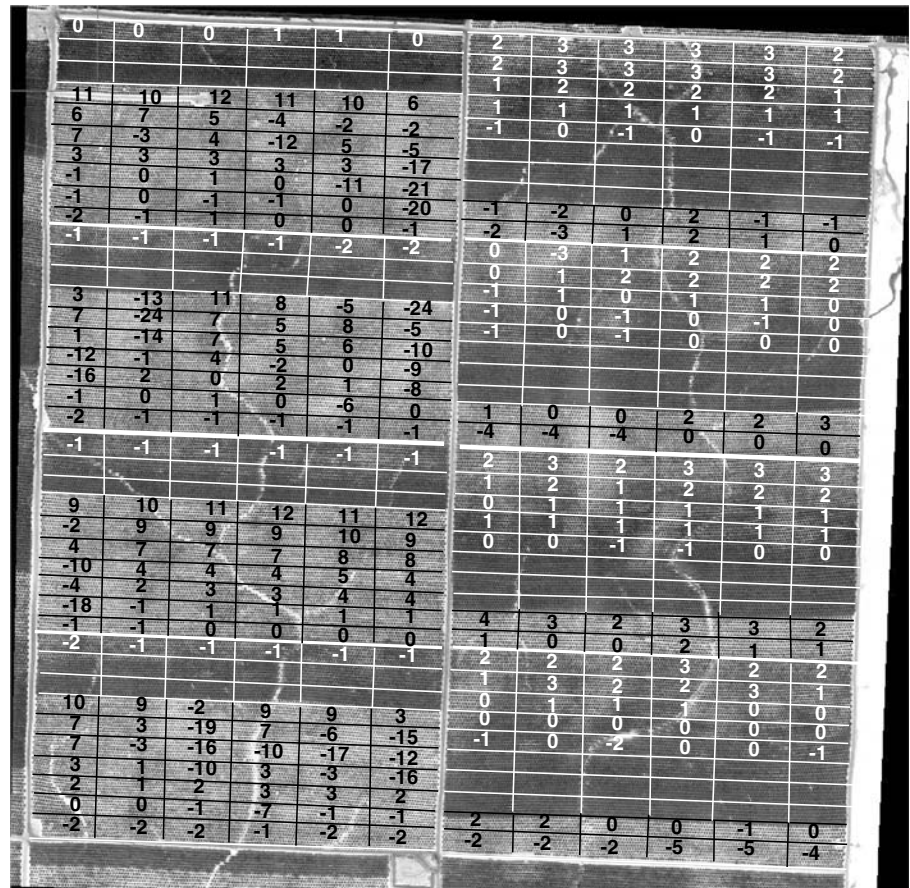
Discussion

The spatial heterogeneity in *CWSI* over the two 130-ha fields, depicted in the map of Fig. 2, provides a measure of irrigation performance based on the crop response to water. Given that trees were of the same age and that the topography did not seem to justify the differences observed, the heterogeneity would be related to variations in either soil

properties or irrigation. In addition to the methods commonly used for the performance evaluation of irrigation systems (Merriam and Keller 1978; Lord and Ayars 2007), the *CWSI*, a proxy of transpiration (Jackson et al. 1981), quantifies the level of stress at the scale of individual trees and thus offers an alternative to conventional methods of irrigation performance assessment. The close correlations found between *CWSI* and the established methods to quantify tree water status and stomatal conductance (Fig. 3) confirm, as in other tree species (Ben-Gal et al. 2009; Berni et al. 2009a; Gonzalez-Dugo et al. 2013), the validity of *CWSI* as a stress indicator. The advantage of using *CWSI* maps for performance evaluation is that the crop integrates in its response all of the environmental variations, such as those due to the spatial variability of soil water properties and to the lack of uniformity in irrigation water distribution, as well as tree factors such as disease, pests, crop load, pruning and genetics. The empirical approach based on the *NWSB* used in this study enabled the calculation of the *CWSI* with a limited meteorological dataset (air temperature and relative humidity, at the time of flights). Nevertheless, its use is restricted to clear days with a vapor pressure deficit above 2 kPa at midday. The analytical approach developed by Jackson et al. (1981) enables the calculation over a wider range of meteorological conditions, although the large input requirements for its calculation (net radiation and aerodynamic resistance) have hampered its use (Maes and Steppe 2012).

One of the objectives of this work was to assess the feasibility of using high-resolution thermal imagery acquired from an unmanned system to quantify the water status of a large farm of over 100 ha in one flight. Other approaches have used thermal sensors installed on the center-pivot system to map the canopy temperature of a whole field as an indicator of water status (Peters and Evett 2004; O'Shaughnessy et al. 2011, 2013). Turnaround time and cost are two factors that should be important when comparing the use of airborne thermal imagery against ground sensors for performance evaluation and for irrigation advisory services. Berni et al. (2009b) first proposed the use of thermal sensors mounted on UAVs for the determination of

Fig. 9 Map of calculated deviation in the irrigation interval according to the spatial analysis



canopy temperatures over large areas at a lower cost than when using ground-based sensors.

The analysis of the mean value of CWSI and its standard deviation at the different levels (tree, unit, set and block; Table 1) reinforced the consistency of the CWSI for monitoring irrigation, as its mean value was maintained within a narrow range for all the scales considered. It also highlighted the importance of the size of the irrigation unit. Large irrigation units absorb the variability that is naturally observed at the tree level. As a result, the standard deviation decreased as irrigation unit size increased. This result was in agreement with Sadler et al. (2002) who recommended the reduction in size of irrigation units as a means for increasing the efficiency of irrigation.

The patterns of CWSI evolution with time were similar for F1 and F2, but the CWSI rose earlier in the case of F2 (Fig. 4). This can be attributed to the 20-day irrigation interval imposed for two irrigation cycles to F2 that, undoubtedly, depleted the soil water reserve relative to that of F1, hence the earlier increase in the CWSI of F2 (Fig. 4). This is also confirmed by the greater rate of change in CWSI in F2 relative to that in F1, as shown in Fig. 5. The negative CWSI values in the first few days after irrigation

are caused by the use of an average baseline for the CWSI calculations, while there are observations above and below the regression line. It should be noted that the observed CWSI patterns as a function of days after irrigation were very similar for the 2 days (of very similar climatic conditions) demonstrating the consistency of the observations and of the method followed for the canopy temperature and CWSI determinations (Fig. 4). A two-flight sequence may be used to confirm the observations of a single flight and to assess the change in CWSI for each management unit as time goes on, in order to construct graphs such as those of Fig. 4, if there is not sufficient variation in the CWSI determined from a single flight.

Once the CWSI values are computed, it is possible to assess the level of water stress of a field. In F2, as the increased irrigation interval was excessive, a significant area of the field was under severe stress 16 days after irrigation (Fig. 6). The lines for the different DSLI of Fig. 6 may be used to decide on the desirable irrigation interval that would keep the majority of the field under a prescribed CWSI value that reflects a desirable stress threshold for the given crop.

Given the consistency in the CWSI values, an average relation between CWSI and DSLI was developed (Fig. 7)

to assess the deviations from the average value of each management unit. The differences in intercept between the two relations are probably due to the differences in stored soil water caused by the different irrigation schedules. The CWSI trend in the areas of F2 which were irrigated more than 10 days ago has a very mild slope (Fig. 7), suggesting that the trees were controlling water loss, and at the same time, they must have been extracting subsoil moisture to keep a stable water deficit. Iniesta et al. (2008) found in the same orchard that pistachio is capable of extracting moisture deep from the subsoil, with substantial extraction from soil layers below 2 m deep.

The distribution of the calculated $\overline{\text{CWSI}}$ is plotted in Fig. 8. For a given unit, the difference between the $\overline{\text{CWSI}}$ and its actual CWSI is a measure of the variability in CWSI. The plot of the cumulative CWSI values against the area represents the overall water status variability of F1 and F2 (Fig. 8). A positive value of $\text{CWSI}_{\text{actual}} - \overline{\text{CWSI}}$ means that the crop water status is better than what would be expected, according to the time elapsed since last irrigation, and thus, it is overirrigated. This could be due to less than average crop transpiration and/or to greater than average stored soil water. The plots in Fig. 8b indicate that about 70 % of F1 is overirrigated and the rest is more stressed than what it should be, while in F2, roughly half of the field is more stressed than what it should be, according to the time elapsed since last irrigation.

One goal of the assessment is to develop an approach for providing precision irrigation recommendations. Once the departure from the $\overline{\text{CWSI}}$ of each irrigation unit has been determined, it is possible to calculate the departure in days of each unit from the farm-fixed schedule, as done in Fig. 9, where the numbers of each unit indicate the difference in days between the average and the specific schedule of each set. To estimate the potential benefits of precision irrigation versus current practice, we calculated an irrigation calendar for F1, from 20 May to 30 September, yielding a total of 11 applications at 10-day intervals, either uniformly across the whole F1 or as variable intervals for all the units where the calculated interval would be greater than 10 days. Assuming that the detected differences in irrigation interval among units were conserved throughout the season, the difference would be equivalent to 15.5 % of the irrigation operating costs, which, in this farm, given its pumping water costs, would be equivalent to a potential savings of \$300 ha⁻¹. To achieve such savings, the irrigation system would have to be reengineered for the autonomous operation of single management units.

Water shortages may force growers to reduce irrigation applications. On a timely basis, F2 applied half of the water depth relative to F1, as irrigation was launched every 2 days instead of daily (although the amount of water applied per irrigation event was the same). Under the conditions of F2,

increasing the accuracy of irrigation scheduling should be even more beneficial than in the case of F1, where differences among irrigation units are smaller (Fig. 9). To assess the potential benefits of precision irrigation, the average yield reduction in the block would have to be compared against the yield reduction in individual units, if they could be operated on a schedule based on their CWSI values. After computing the seasonal AW, a water production function could be used to estimate the yield reduction for each unit, relative to the average yield reduction in the block.

Conclusions

This work demonstrates that the CWSI derived from high-resolution thermal imagery acquired from unmanned systems is a valuable tool for assessing the spatial variability of crop water status in a commercial pistachio orchard and that it can be used for precision irrigation. Based on two flights carried out on different days, a methodology was developed, whereby the difference between the average CWSI for all the units that were irrigated on the same day and the actual CWSI of each individual unit was used for assessing the overirrigation or underirrigation that result from a fixed irrigation scheduling. By converting the difference in CWSI into days, it was possible to determine an optimal irrigation interval for every unit.

The high-resolution CWSI determinations were able to discriminate between the two blocks that differed in irrigation frequency, and it was found that the increase in CWSI with time after irrigation followed the same trend in the two blocks. Under the hypothesis of stable state conditions during the central part of the summer, calculations were performed to simulate scenarios to assess the possible benefits of precision irrigation. Our results indicated that by changing from the present irrigation system to a variable-rate irrigation system, over 15 % of irrigation costs could be saved.

Acknowledgments We acknowledge the contribution of Dr. J.A.J. Berni and Dr. L. Suarez during the field campaigns and Dr. Notario, A. Vera, M. Salinas and K. Brooks for their technical support. Chris Wylie and Richard Paslay, from Agri-World Cooperative, are also acknowledged. This work was funded by the Spanish Ministry of Science and Innovation (CONSOLIDER CSD2006-0067 and AGL2009-13105).

References

- Ambast SK, Keshari AK, Gosain AK (2002) Satellite remote sensing to support management of irrigation systems: concepts and approaches. *Irrig Drain* 51(1):25–39
- Bellvert J, Zarco-Tejada PJ, Girona J, Fereres E (2014) Mapping crop water stress index in a “Pinot Noir” vineyard: comparing ground

- measurements with thermal remote sensing imagery from an unmanned aerial vehicle. *Precis Agric* 15:361–376
- Ben-Gal A, Agam N, Alchanatis V, Cohen Y, Yermiyahu U, Zipori I, Presnov E, Sprintsin M, Dag A (2009) Evaluating water stress in irrigated olives: correlation of soil water status, tree water status, and thermal imagery. *Irrig Sci* 27:367–376
- Berni JAJ, Zarco-Tejada PJ, Sepulcre-Canto G, Fereres E, Villalobos F (2009a) Mapping canopy conductance and CWSI in olive orchards using high resolution thermal remote sensing imagery. *Remote Sens Environ* 113:2380–2388
- Berni JAJ, Zarco-Tejada PJ, Suarez L, Fereres E (2009b) Thermal and narrowband multispectral remote sensing for vegetation monitoring from an unmanned aerial vehicle. *IEEE Trans Geosci Remote Sens* 47(3):722–738
- Bonachela S, Orgaz F, Villalobos FJ, Fereres E (2001) Soil evaporation from drip-irrigated olive orchards. *Irrig Sci* 20(2):65–71
- Bresler E (1977) Trickle-drip irrigation: principles and application to soil-water management. *Adv Agron* 29:343–393
- Evans RG, Sadler EJ (2008) Methods and technologies to improve efficiency of water use. *Water Resour Res* 44:W00E04. doi:10.1029/2007WR006200
- Goldhamer DA, Fereres E (2001) Simplified tree water status measurements can aid almond irrigation. *Calif Agric* 55(3):32–38
- Gonzalez-Dugo V, Zarco-Tejada P, Berni JAJ, Suarez L, Goldhamer D, Fereres E (2012) Almond tree canopy temperature reveals intra-crown variability that is water stress-dependent. *Agric For Meteorol* 154–155:156–165
- Gonzalez-Dugo V, Zarco-Tejada P, Nicolas E, Nortés PA, Alarcon JJ, Intrigliolo DS, Fereres E (2013) Using high resolution UAV thermal imagery to assess the variability in the water status of five fruit tree species within a commercial orchard. *Precis Agric* 14(6):660–678
- Hsiao TC (1990) Measurement of plant water status. In: Stewart BA, Nielsen DC (eds) *Irrigation of agriculture crops*, vol special publication no. 30. Am Soc Agron, Madison, WI, USA, pp 243–279
- Idso SB, Jackson RD, Pinter PJ Jr, Reginato RJ, Hatfield JL (1981) Normalizing the stress-degree-day parameter for environmental variability. *Agric Meteorol* 24:45–55
- Iniesta F, Testi L, Goldhamer D, Fereres E (2008) Quantifying reductions in consumptive water use under regulated deficit irrigation in pistachio (*Pistachia vera* L.). *Agric Water Manag* 95:877–886
- Jackson RD, Reginato RJ, Idso SB (1977) Wheat canopy temperature: a practical tool for evaluating water requirements. *Water Resour Res* 13(3):651–656
- Jackson R, Idso S, Reginato R, Pinter PJ (1981) Canopy temperature as a crop water stress indicator. *Water Resour Res* 17:1133–1138
- Jury WA, Vaux HR (2007) The emerging global water crisis: managing scarcity and conflict between water users. *Adv Agron* 95:1–76
- Kravchenko AN, Robertson GP, Thelen KD, Harwood RR (2005) Management, topographical and weather effects on spatial variability of crop grain yields. *Agron J* 97:514–523
- Lee WS, Alchanatis V, Yang C, Hirafuji M, Moshou D, Li C (2010) Sensing technologies for precision specialty crop production. *Comp Electron Agric* 74:2–33
- Lord JM, Ayars JE (2007) Evaluating performance. In: Hoffman GJ, Evans RG, Jensen ME, Martin DL, Elliot RL (eds) *Design and operation of farm irrigation systems*. ASABE, St. Joseph, MI, USA, pp 791–803
- Maes WH, Steppe K (2012) Estimating evapotranspiration and drought stress with ground-based thermal remote sensing in agriculture: a review. *J Exp Bot* 63(13):4671–4712
- Martin DI, Stegman EC, Fereres E (1990) Irrigation scheduling principles. In: Hoffman GJ (ed) *Management of farm irrigation systems*. ASAE, St. Joseph, pp 105–203
- Merriam JL, Keller J (1978) *Farm irrigation system evaluation: a guide for management*. Utah State University, Logan
- Molden D (2007) *Water for food, water for life: a comprehensive assessment of water management in agriculture*. International Water Management Institute, London
- Moran MS, Clarke TR, Inoue Y, Vidal A (1994) Estimating crop water deficit using the relation between surface-air temperature and spectral vegetation index. *Remote Sens Environ* 49(3):246–263
- O'Shaughnessy SA, Evett SR, Colaizzi PD, Howell TA (2011) Using radiation thermography and thermometry to evaluate crop water stress in soybean and cotton. *Agric Water Manag* 98(10):1523–1535
- O'Shaughnessy SA, Evett SR, Colaizzi PD, Howell TA (2013) Wireless sensor network effectively controls center pivot irrigation of sorghum. *Appl Eng Agric* 29(6):853–864
- Peters RT, Evett SR (2004) Complete center pivot automation using the temperature-time threshold method of irrigation scheduling. ASAE paper no. 042096. St. Joseph, MI
- Rodriguez D, Robson AJ, Belford R (2009) Dynamic and functional monitoring technologies for applications in crop management. In: Sadras VO, Calderini D (eds) *Crop physiology. Applications for genetic improvement and agronomy*. Elsevier, Amsterdam, pp 489–510
- Sadler EJ, Camp CR, Evans DE, Millen JA (2002) Spatial variation of corn response to irrigation. *Trans Am Soc Agric Eng* 45(6):1869–1881
- Testi L, Goldhamer D, Iniesta F, Salinas M (2008) Crop water stress index is a sensitive water stress indicator in pistachio trees. *Irrig Sci* 26:395–405
- Zarco-Tejada PJ, Gonzalez-Dugo V, Berni JAJ (2012) Fluorescence, temperature and narrow-band indices acquired from a UAV platform for water stress detection using a micro-hyperspectral imager and a thermal camera. *Remote Sens Environ* 117:322–337
- Zarco-Tejada PJ, Gonzalez-Dugo V, Williams LE, Suarez L, Berni JAJ, Goldhamer D, Fereres E (2013) A PRI-based water stress index combining structural and chlorophyll effects: assessment using diurnal narrow-band airborne imagery and the CWSI thermal index. *Remote Sens Environ* 138:38–50
- Zhang N, Wang M, Wang N (2002) Precision agriculture—a worldwide overview. *Comp Electron Agric* 36(2–3):113–132